

A CORAVEL radial-velocity monitoring of giant Ba and S stars: spectroscopic orbits and intrinsic variations (I)^{*}

S. Udry¹, A. Jorissen², M. Mayor¹ and S. Van Eck^{1,2}

¹Observatoire de Genève, CH-1290 Sauverny, Switzerland

²Institut d'Astronomie et d'Astrophysique, Université Libre de Bruxelles, C.P.226, Bvd du Triomphe, B-1050 Bruxelles, Belgium

Received date; accepted date

Abstract. With the aim of deriving the binary frequency among Ba and S stars, 56 new spectroscopic orbits (46 and 10, respectively) have been derived for these chemically-peculiar red giants monitored with the CORAVEL spectrometers. These orbits are presented in this paper (38 orbits) and in a companion paper (Udry et al. 1998, Paper II; 18 orbits). The results for 12 additional long-period binary stars (6 and 6, respectively), for which only minimum periods (generally exceeding 10 y) can be derived, are also presented here (10) and in Paper II (2). The global analysis of this material, with a few supplementary orbits from the literature, is presented in Jorissen et al. (1998).

For the subsample of Mira S, SC and (Tc-poor) C stars showing intrinsic radial-velocity variations due to atmospheric phenomena, orbital solutions (when available) have been retained if the velocity and photometric periods are different (3 stars). However, it is emphasized that these orbit determinations are still tentative. Three stars have been found with radial-velocity variations synchronous with the light variations. *Pseudo*-orbital solutions have been derived for those stars. In the case of RZ Peg, a line-doubling phenomenon is observed near maximum light, and probably reflects the shock wave propagating through the photosphere.

Key words: Stars: late-type – Stars: barium – Stars: S – Stars: Mira – Binaries: spectroscopic

1. Introduction

Several samples of chemically-peculiar red giants (PRG) were monitored in radial velocity with the aim of deriv-

ing their binary frequency. The spectroscopic-binary orbits presented here and in a companion paper (Udry et al. 1998, Paper II) belong to a systematic survey of barium and Tc-poor S stars undertaken to gain insight into the formation process of these stars.

Barium stars and their Pop. II counterparts, the CH stars, are not evolved enough to have produced on their own the observed overabundances of elements heavier than Fe (e.g. Lambert 1985), usually associated with the nucleosynthesis occurring during He-burning thermal pulses on the asymptotic giant branch (AGB). The binary nature of these stars accounts for the observed chemical peculiarities through mass transfer across the binary system (McClure et al. 1980; McClure 1983). The exact mass-transfer mode is still a matter of debate but is turning towards a solution involving Roche-lobe overflow or wind accretion, depending on the orbital period (Han et al. 1995).

Contrarily to Tc-rich S stars which are able to synthesize heavy elements on their own, Tc-poor S stars are believed to be the cool descendants of barium stars and thus also owe their chemical peculiarities to binarity (Jorissen & Mayor 1992; Ake 1997; Van Eck et al. 1997).

The 46 new (43) or updated (3) spectroscopic orbits of barium stars (+ 6 Ba stars with P_{\min} determinations) and the 10 new orbits of S stars (+ 6 binary S stars with P_{\min} determinations) reported in this paper and in Paper II, combined with a few other newly available orbits (see references in Jorissen et al. 1998), provide an unequalled sample to constrain the binary evolution channels relevant for barium stars, as identified by Han et al. (1995) using only 17 barium-star orbits. It also allows us to re-discuss the evolutionary link between barium and Tc-poor S stars. This is done in a companion paper (Jorissen et al. 1998).

In order not to bias the S-star sample towards low luminosities, a small sample of S Miras, SC and Tc-poor C stars were also monitored. However, the radial-velocity jitter associated with atmospheric motions (envelope pul-

Send offprint requests to: S. Udry

^{*} Based on observations obtained at the Haute-Provence Observatory (France) and at the European Southern Observatory (ESO, La Silla, Chile)

sation, large convective cells, shocks) induces non-orbital radial-velocity variations that limit our ability to detect binaries and, *a fortiori*, to derive their orbital elements, at a given level of measurement precision. Illustrative examples will be discussed at the end of the paper.

This paper is organized as follows. Section 2 describes the stellar samples. The observations are briefly discussed and a short statistical overview of the survey is given in Sect. 3. Section 4 provides the orbital elements and the radial-velocity curves. Some stars are also commented individually. Mira S, SC and C stars with radial-velocity variations associated or not with an orbital motion are discussed in Sect. 5.

2. CORAVEL star samples and binary content

The star samples considered in this paper were observed with the CORAVEL spectro-velocimeters (Baranne et al. 1979) installed on the 1-m Swiss telescope at the Haute-Provence Observatory (France) and on the 1.54-m Danish telescope at the European Southern Observatory (La Silla, Chile). The criteria defining these various samples, their monitoring history and their binary content are described in the following subsections. For a detailed discussion of the binary frequency in the corresponding PRG family as a whole, we refer to the analysis paper (Jorissen et al. 1998).

2.1. Strong barium stars

This sample includes the 28 barium stars with a strong anomaly (Ba4 or Ba5 on the scale defined by Warner 1965) from the list of Lü et al. (1983), not already monitored by McClure at the Dominion Astrophysical Observatory (DAO), plus the special star HD 46407 (see Sect. 2.4). These stars are presented in Table 1. The CORAVEL monitoring of that sample started in 1984 (preliminary results were presented in Jorissen & Mayor 1988). All the stars show radial-velocity variations due to binary motion except HD 19014 for which the situation is still unclear. Among the new spectroscopic orbits of strong barium stars, 18 are presented in Sect. 4. The others can be found in Paper II (8), in Griffin et al. (1996; 2) and in Jorissen et al. (1995; 1). The corresponding references are indicated in the last column of the table.

2.2. Mild barium stars

A random selection of 33 stars with a mild barium anomaly (Ba<1, Ba1, Ba2 on the Warner scale, from the list of Lü et al. 1983) has been monitored since 1988 for comparison. A few mild barium stars observed by the Marseille team (see Paper II) for a different purpose were included in our initial sample later on. The global sample, also including 3 DAO stars (see next section), is presented in Table 2.

Table 1. The sample of barium stars with strong anomalies (Ba4 or Ba5 on the scale defined by Warner 1965) monitored with CORAVEL. The spectral type, visual magnitude and $B - V$ index are from Lü et al. (1983) or, if not available, from Lü (1991). The last column refers to a note at the end of the table providing the reference where the orbital elements are to be found

HD/DM/..	Sp.	Ba	V	$B - V$	orbit
5424	K1	4	9.48	1.14	1
19014	K4	5	8.18	1.69	0
20394	K0	4	8.72	1.09	6
24035	K4	4	8.48	1.24	1
36598	K2	4	8.02	1.31	1
42537	K4	5	8.93	1.85	1
43389	K2	5	8.32	1.48	2
44896	K3	5	7.26	1.58	2
46407 ^a	K0	3	6.28	1.12	2
50082	K0	4	7.42	1.02	2
60197	K3	5	7.74	1.69	1
84678	K2	4	9.00	1.46	1
88562	K2	4	8.54	1.42	1
92626	K0	5	7.10	1.34	2
100503	K3	5	8.74	1.69	1
107541	K0	4	9.39	1.06	2
120620	K0	4	9.62	1.10	1
121447 ^c	K7	5	7.85	1.75	7
123949	K6	4	8.73	1.37	1
154430	K2	4	8.74	1.56	1
196445	K2	4	9.08	1.42	1
201657	K1	4	8.04	1.22	2
201824	K0	4	8.91	1.08	6
211594	K0	4	8.11	1.16	2
211954	K2	5	10.21	1.33	1
+38° 118	K2	5	8.88	1.50	1
-42° 2048	K2	4	9.30	1.41	1
-64° 4333 ^d	K0	4	9.60	1.20	1
Lü 163	G5	5	10.90	1.18	1

^a) DAO+CORAVEL measurements

^c) Two classifications: Ba5 or S0. Appears in both tables

^d) CpD

References to orbital elements: 0: Jorissen et al. (1998);

1: this paper; 2: Udry et al. (1998, Paper II); 6: Griffin et al.

(1996); 7: Jorissen et al. (1995)

Among these mild barium stars, 27 stars are definitely binaries (3 with fixed parameters, and 6 with only a lower limit available on the orbital period), 3 are suspected binaries, 4 show no evidence of binary motion and 2 (HD 65699 and HD 206778) are supergiants misclassified as mild barium stars (Smith & Lambert 1987; superscript 'b' in Table 2). Results for 14 mild barium stars are presented in Sect. 4. The remaining 13 binaries are to be found in Paper II (12) and in Griffin (1991; 1).

Table 2. The sample of barium stars with mild anomalies (Ba<1, Ba1, Ba2 on the scale defined by Warner 1965) monitored with CORAVEL. The spectral type, visual magnitude and $B - V$ index are from Lü et al. (1983) or, if not available, from Lü (1991). Column 6 gives a binarity flag (o: orbit, po: preliminary orbit with fixed parameters, mp: minimum period only available, sb: suspected binary, c: no radial-velocity variation). The last column refers to a note at the end of the table providing the reference where the orbital elements are to be found

HD/DM	Sp.	Ba	V	$B - V$	bin.	orbit
18182	K0	< 1	8.95	1.01	sb	0
22589	G5	< 1	9.00	0.72	po	1
26886	G8	1	7.97	0.97	o	2
27271	G8	1	7.49	1.00	o	2
40430	K0	1	8.07	1.01	mp	1
49841	G8	1	8.56	0.99	o	2
50843	K1	1	8.13	1.06	c	0
51959	K2	1	8.95	1.06	mp	1
53199	G8	2	9.08	0.95	po	2
58121	K0	1	7.93	1.14	o	2
59852	G9	1	8.67	0.92	po	1
65699 ^b	G5	1	5.07	1.12		0
91208	K0	1	8.02	0.95	o	1
95193	K0	1	8.28	0.99	o	1
95345	K2	1	4.83	1.16	c	0
101079	K1	1	8.43	0.96	mp	2
104979	K0	1	4.16	0.99	mp	2
119185	K0	1	8.91	1.00	c	0
130255	K0	1	8.61	1.08	c	0
131670 ^a	K1	1	8.00	1.20	o	1
134698	K1	1	8.72	1.31	mp	1
139195	K1	1	5.26	0.95	o	12
143899	G8	1	8.30	1.08	o	1
180622	K1	1	7.62	1.23	o	2
183915	K0	2	7.28	1.34	sb	0
196673 ^a	K2	2	6.98	1.12	o	1
200063	K3	1	7.31	1.60	o	2
206778 ^b	K2	< 1	2.38	1.52		0
210946	K1	1	8.07	1.08	o	2
216219	G5	1	7.45	0.74	o	2
218356	K2	2	4.47	1.35	sb	0
223617 ^a	K2	2	6.94	1.16	o	2
288174	K0	1	8.99	1.24	o	1
-01°3022	K1	1	9.25	1.09	o	1
-10°4311	G0	1	9.89	0.63	mp	1
-14°2678	K0	< 1	9.81	0.99	o	1

a) DAO+CORAVEL measurements

b) misclassified as mild Ba star

References to orbital elements: 0: Jorissen et al. (1998);

1: this paper; 2: Paper II; 12: Griffin (1991)

2.3. DAO stars

For several barium stars monitored by McClure, a few recent CORAVEL measurements, obtained in the framework of other projects, are nevertheless available. These new

measurements often allow us to improve the DAO orbit, since they significantly increase the span of the monitoring. All these new orbital parameters are used in the analysis paper (Jorissen et al. 1998). The present paper and Paper II provide only four of these stars, 3 for which the number of CORAVEL measurements is fairly large (HD 46407, HD 131670 and HD 223617) and 1 (HD 196673) for which the 2 new available observations significantly change the period obtained by McClure & Woodsworth (1990). These stars are also included in Tables 1 and 2, where they are identified by superscript 'a' in column 1. Their orbits are presented in Sect. 4 or in Paper II.

2.4. Two barium stars of special importance

The K0Ba3 star HD 46407 and K2Ba2 star HD 218356 (=56 Peg) were included in the CORAVEL samples (Tables 1 and 2) because of their unique photometric behaviour among barium stars. HD 46407 exhibits long-term photometric variations in phase with the orbital motion (Jorissen et al. 1991; Jorissen 1997), whereas 56 Peg is a strong X-ray and UV source, indicating that it is an interacting binary system possibly hosting an accretion disk (Schindler et al. 1982; Dominy & Lambert 1983). A combined DAO/CORAVEL orbit of HD 46407 is presented in Paper II whereas no clear orbital solution emerges for 56 Peg yet.

2.5. Non-variable S stars

An initial sample of 9 S stars, whose monitoring started in 1984 (with preliminary results presented in Jorissen & Mayor 1988, 1992) was extended to 36 stars in 1988. This sample contains bright northern S stars from the *General Catalogue of Galactic S Stars* (GCGSS; Stephenson 1984) with no variable star designation, neither in the *General Catalogue of Variable Stars* (Kholopov et al. 1985) nor in the *New Catalogue of Suspected Variable Stars* (Kukarkin et al. 1982). The criterion of photometric stability has been adopted to avoid the confusion introduced by the envelope pulsations masking the radial-velocity variations due to orbital motion. Such a selection criterion clearly introduces a strong bias against intrinsically bright S stars.

The sample of 36 photometrically non-variable S stars is presented in Table 3. Among them, 24 are binaries¹ (6 have only a lower limit available on the orbital period), 10 show no evidence for binary motion, and 2 (HD 262427 and BD +22°4385) are likely misclassified (Jorissen et al. 1998). The new spectroscopic binaries (18) are described in Sect. 4 (16) and in Carquillat et al. (1998; 2).

¹ including HD 121447 already presented in the strong barium sample

Table 3. The sample of photometrically non-variable S stars monitored with CORAVEL. The spectral type is from the GCGSS. The V magnitude and $B-V$ index for S stars are from various sources, as listed in *The General Catalogue of Photometric Data* (GCPD; Mermilliod et al. 1997). In case no data are listed in the GCPD, the V magnitude from the GCGSS is listed. Column 6 gives a binarity flag (o: orbit, po: preliminary orbit with fixed parameters, mp: minimum period only available, j: jitter, c: no radial-velocity variation). The last column refers to a note at the end of the table providing the reference where the orbital elements are to be found

HD/DM	GCGSS	Sp.	V	$B-V$	bin.	orbit
7351	26	S3/2	6.43	1.70	o	3
30959	114	S3/1	4.74	1.84	mp	1
35155	133	S4,1	6.77	1.80	o	0,10
49368	260	S3/2	7.65	1.78	o	1
61913	382	M3S	5.56	1.64	j	0
63733	411	S4/3	7.94	1.74	o	1
95875	720	S3,3	8.74	1.11	o	1
121447 ^c	–	S0	7.85	1.75	o	1
170970	1053	S3/1	7.60	2.00	o	1
184185	1140	S3*4	9.20	2.00	mp	1
189581	1178	S4*2	8.70	2.00	j	0
191226	1192	M1-3S	7.34	1.32	o	3
191589	1194	S	7.70	2.00	o	1
192446	1198	S6/1	9.80	2.00	j	0
216672	1315	S4/1	6.36	1.80	j	0
218634	1322	M4S	5.03	1.47	mp	1
246818	156	S	9.60	2.00	o	1
262427 ^b	247		9.90	2.00		0
288833	233	S3/2	9.40	1.91	mp	1
332077	1201	S3,1	9.00	1.96	o	10
343486	1092	S6,3	–	2.00	o	1
+04° 4354	1193	S4*3	9.50	2.00	j	0
+15° 1200	219	S4/2	9.39	2.01	j	0
+20° 4267	1158	Swk	10.80	2.55	j	0
+21° 255	45	S3/1	8.60	1.30	o	1
+22° 700	96	S6,1	10.50	2.00	o	10
+22° 4385 ^b	1271		10.10	2.00		0
+23° 3093	981	S3/3	9.90	2.00	o	10
+23° 3992	1209	S3,3	10.50	2.00	o	1
+24° 620	87	S3/3	8.88	2.06	o	10
+28° 4592	1334	S2/3:	9.50	1.40	o	1
+31° 4391	1267	S2/4	9.30	2.00	mp	1
+79° 156	106	S4/2	10.10	1.70	mp	1
−04° 2121	416	S5/2	9.20	2.00	j	0
−10° 1334	176	Sr	9.00	2.00	j	0
−21° 2601	554	S3*3	9.20	2.00	j	0

^b) star misclassified as S?

^c) Two classifications: Ba5 or S0. Appears in both tables
References to orbital elements: 0: Jorissen et al. (1998); 1: this paper; 3: Carquillat et al. (1998); 10: Jorissen & Mayor (1992)

2.6. Mira S stars, SC stars and Tc-poor carbon stars

A sample of 13 Mira S stars (Table 4) has also been monitored in order not to restrict the search for binaries to

Table 4. The sample of Mira S stars, SC stars and C stars with no Tc lines, monitored with CORAVEL. The spectral type is from the GCGSS, and $B-V$ from the GCPD

HD/DM	GCGSS	Var	Sp.	$B-V$
1967	9	R And	S5-7/4-5e	1.97
4350	12	U Cas	S5/3e	2.00
14028	49	W And	S7/1e	1.70
29147	103	T Cam	S6/5e	2.30
53791	307	R Gem	S5/5	2.10
70276	494	V Cnc	S3/6e	2.20
110813	803	S UMa	S3/6e	2.10
117287	–	R Hya	M6e-M9eS	1.60
185456	1150	R Cyg	S6/6e	2.00
187796	1165	χ Cyg	S7/1.5e	1.80
190629	1188	AA Cyg	S6/3	1.80
195763	1226	Z Del	S4/2e	2.00
211610	1292	X Aqr	S6,3e:	2.00
286340	117	GP Ori	SC7/8	2.90
44544	212	FU Mon	S7/7	3.00
−04° 1617	244	V372 Mon	SC7/7	2.50
−08° 1900	344		S4/6	1.90
54300	–	R CMi	CS	2.50
198164	–	CY Cyg	CS	2.00
209890	–	RZ Peg	CS	3.90
46687	–	UU Aur	C no Tc	3.00
76221	–	X Cnc	C no Tc	3.36
108105	–	SS Vir	C no Tc	3.00

low-luminosity S stars (see Sect. 2.5). However, the envelope pulsations of Mira stars seriously hamper that search by causing a substantial radial-velocity jitter. This will be discussed in Sect. 5.

A sample of 7 SC and CS stars suffering the same problem has been monitored as well with CORAVEL, along with the 3 carbon stars lacking Tc from the list of Little et al. (1987). These stars are also listed in Table 4. Radial-velocity variations are observed for all these stars.

In case the photometric and radial-velocity periods are different, a *tentative* orbital solution is proposed. The results are presented in Sect. 5.

3. Observations and overview of the survey

Since 1983, more than 2500 measurements have been gathered for the stars of the samples described above. The radial velocities are obtained by usual cross-correlation (cc) and gaussian-fitting techniques (see Baranne et al. 1979 or Duquenooy et al. 1991 for details). An illustrative example of a profile obtained for HD 24035 (cc-dip with the fitted gaussian) is displayed in Fig. 1a.

The still unpublished individual measurements will be available at the *Centre de Données Stellaires* (CDS) in Strasbourg or on our dedicated web page (obswww.unige.ch/~udry/cine/barium/barium.html) and thus will not appear here.

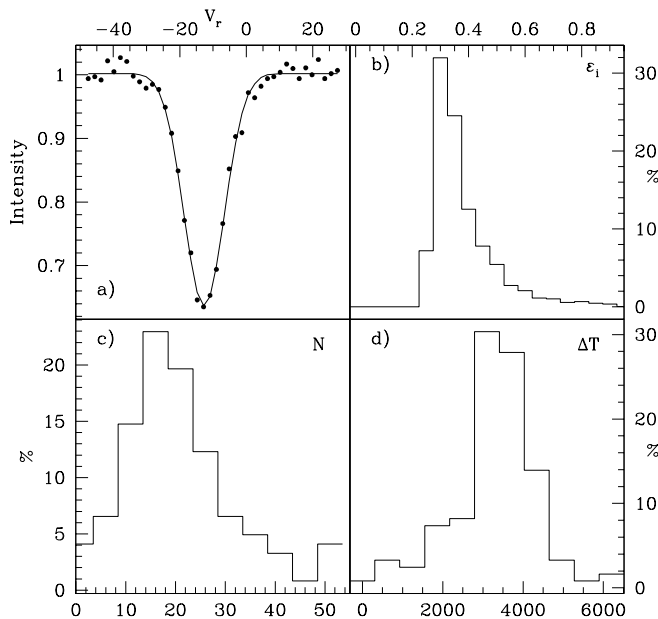


Fig. 1. Statistical overview of the combined samples of barium and S stars: a) typical cross-correlation profile (here an observation of HD 24035); b) distribution of individual measurement errors ε_i (in km s^{-1}); c) distribution of the number of CORAVEL measurements per star N ; d) distribution of spans in days (ΔT) between the first and the last measurements, for every star

The mean precision of the measurements is about 0.3 km s^{-1} (more than 76% of the measurements between 0.25 and 0.4 km s^{-1}) as shown in Fig. 1b displaying the distribution of individual errors ε_i . S stars with non-orbital radial-velocity variations usually present non-gaussian cc-dips (see Sect. 5.1) leading to non-realistic error estimates that slightly swell the upper tail of the distribution. Stars with broad cc-dip widths act in the same way.

The distributions of the number of observations and of the time span of the observations for every star are given in Figs. 1c and 1d, respectively. They illustrate the large observational effort devoted to these programmes. The median value for the number of observations per star is $\overline{N} = 19$ which permits a good estimate of the orbital parameters. The typical span ($\overline{\Delta T} = 3398 \text{ d}$) is about 10 years ensuring a good completeness of the orbital periods up to this value.

Further information on the CORAVEL observation and reduction techniques can be found in Duquenooy et al. (1991).

4. Radial-velocity curves and orbital parameters

The radial-velocity monitoring of a binary star may lead to different qualitative results depending on the param-

eters of the orbital solution (period P , eccentricity e , amplitude K), the number of measurements or the observation sampling. The strategy for the presentation of the results will thus depend on these different cases. Situations possibly encountered are the following:

1) A stable solution is found and the orbital parameters can be derived (flag ‘o’ in Tables 2 and 3). This is the case for most of the orbits presented in this paper. A table is provided with the orbital parameters and their uncertainties and a few additional interesting related quantities as the number of measurements (N) used to derive the orbital solution or the residue ($O - C$) around this solution. The phase-folded orbital solution is then also displayed. Badly constrained parameters are readily identifiable by their large uncertainties.

2) The orbital solution exists but is not fully constrained. One or several parameters (usually P or e) have to be fixed (e.g. for an uncompletely-covered orbit or when the periastron passage in an eccentric orbit has been missed; flag ‘po’ in Tables 2 and 3). In such a case, the adequate orbital parameter is fixed to a probable value as given by the orbital solution with minimum residuals. The obtained *minimized* orbital elements are given in the same table as for case 1) but with no uncertainties on the fixed parameter(s). A diagram with the velocity measurements folded in phase is also provided.

3) The star has a clearly variable radial velocity but the period is insufficiently covered (usually just a drift is observed) to derive a preliminary orbit, even with fixed parameters (flag ‘mp’ in Tables 2 and 3). No solution is found. The minimum period ($P > P_{\min}$) is indicated in the table of orbital elements, along with the number of measurements and the time span of the observations. The figure only displays radial velocities as a function of Julian date. In addition to the individual measurements available at the CDS (Sect. 3), the analysis paper (Jorissen et al. 1998) summarizes the interesting averaged quantities (radial velocity and corresponding uncertainty, etc.) for these stars.

4) No orbital solution can be found because of other sources of radial-velocity variations (jitter, flag ‘j’ in Table 3) masking a possible orbital motion. Average quantities are given in Jorissen et al (1998).

In the following subsections the results for the various star samples described in Sect. 2 will be presented and discussed in turn.

4.1. Strong barium stars

Definitive or preliminary orbits have been obtained for all strong barium stars except HD 19014. The orbital parameters are given in Table 5. For two uncompletely-covered orbits (HD 123949 and HD 211954), the periods have been fixed to *minimized* values (see item 2 above). In 8 cases, even though the Lucy-Sweeney test was compatible with a circular orbit at a 5% confidence level (Lucy & Sweeney

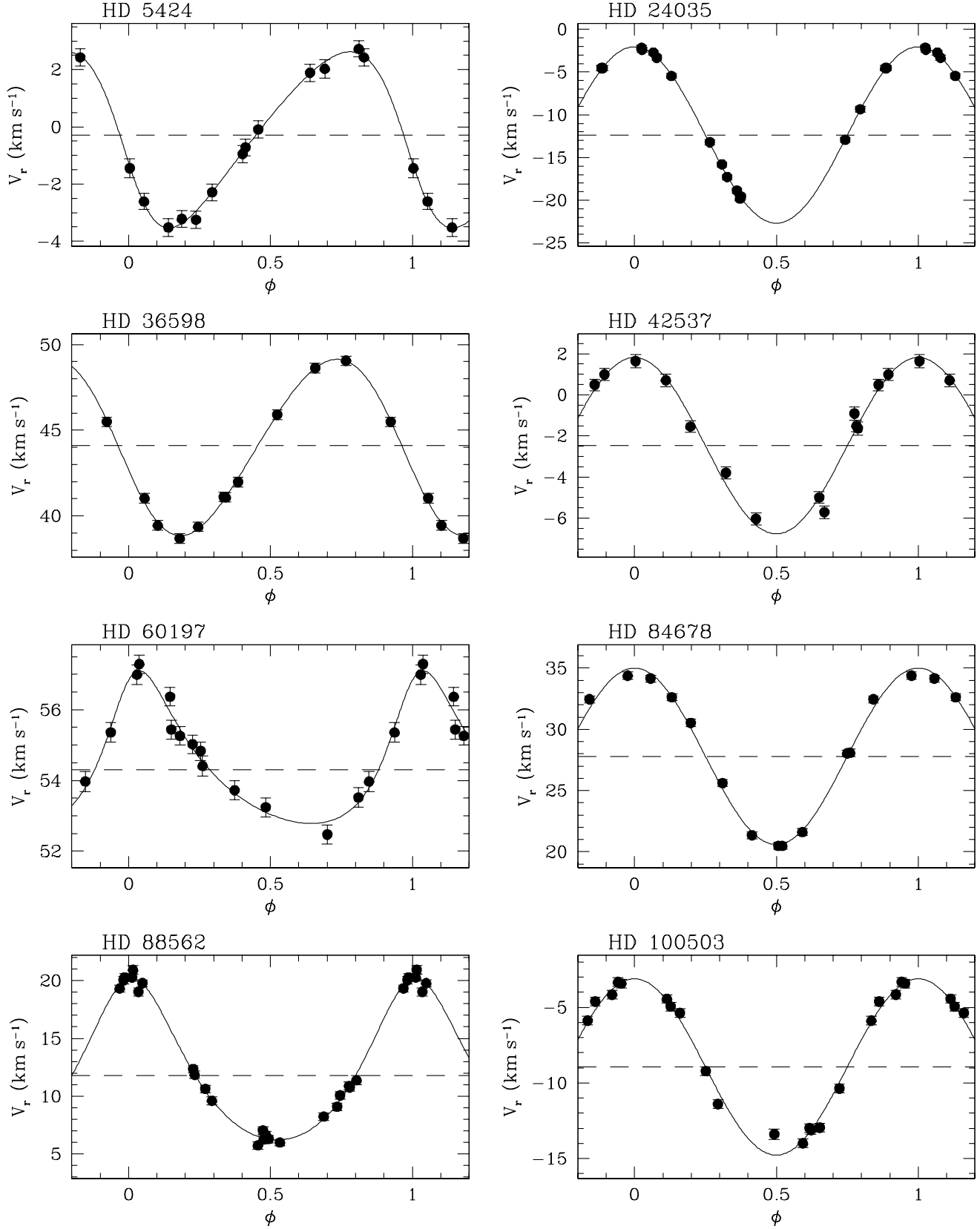


Fig. 2. Phase-folded radial-velocity curves for the strong barium stars. *Minimized* periods (see item 2 in Sect. 4) were fixed for HD 123949 and HD 211954 because of the non-complete coverage of the orbits. BD+38°118 is a triple hierarchical system

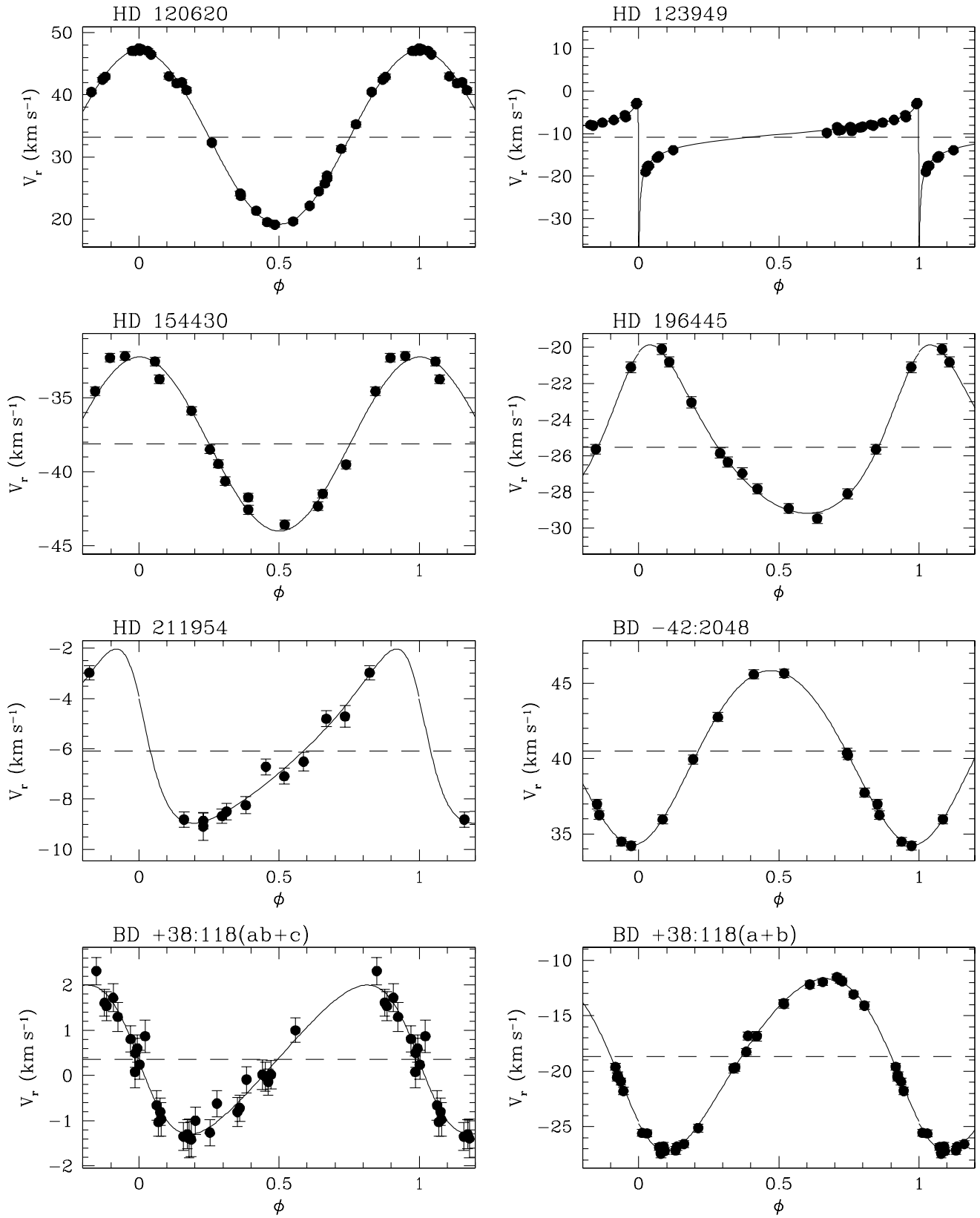


Fig. 2. (continued)

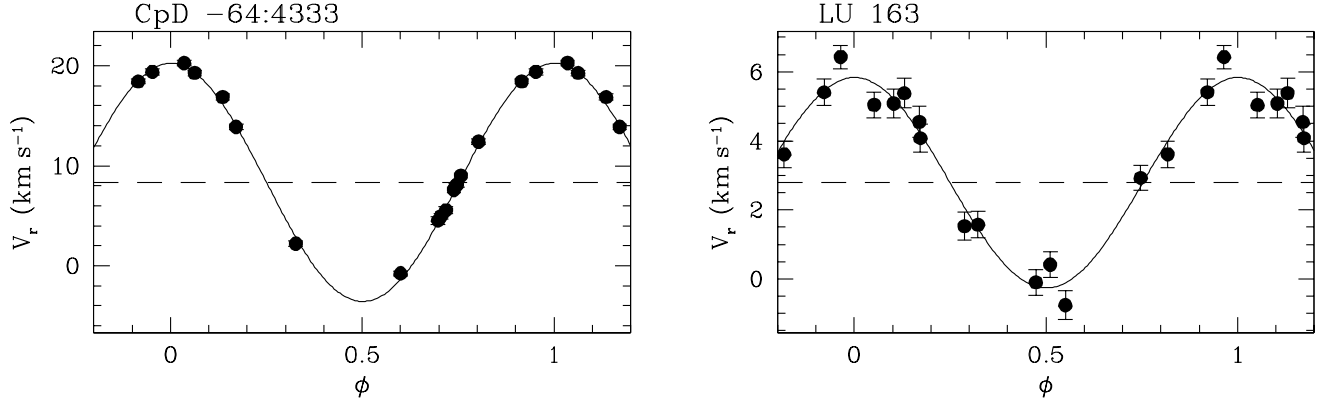


Fig. 2. (continued)

Table 5. Orbital elements for strong barium stars. No uncertainties are given for fixed parameters. The symbol $>$ is used for uncertainties exceeding the parameter values in case of badly constrained orbits. N is the number of measurements used to derive the orbital solution and $O - C$ the residue around this solution. ΔT is the span of the observations

Id HD/DM/..	P [days]	T [HJD -2400000]	e	γ [km s $^{-1}$]	ω [deg]	K [km s $^{-1}$]	$f(m)$	$a \sin i$ [Gm]	N	$O - C$ [km s $^{-1}$]	ΔT [days]
5424	1881.53 18.59	46202.80 34.86	0.226 0.036	-0.28 0.05	104.63 5.87	3.08 0.08	5.281e-03 4.221e-04	77.64 2.19	13	0.180	3306
24035	377.82 0.35	48842.65 26.14	0.020 0.010	-12.51 0.13	214.82 24.76	10.64 0.27	4.725e-02 3.544e-03	55.27 0.14	15	0.186	3271
36598	2652.81 22.66	45838.95 107.50	0.084 0.018	44.10 0.07	104.59 13.96	5.15 0.09	3.715e-02 2.060e-03	187.06 3.77	11	0.210	3270
42537	3216.22 54.68	46147.32 162.50	0.156 0.047	-2.47 0.16	237.61 19.27	4.40 0.25	2.741e-02 4.722e-03	192.18 11.46	12	0.432	3270
60197	3243.76 66.34	46015.97 98.30	0.340 0.051	54.30 0.10	330.94 10.89	2.16 0.13	2.829e-03 5.542e-04	90.66 6.17	14	0.309	3970
84678	1629.91 10.38	44512.25 81.44	0.062 0.020	27.92 0.11	190.00 17.94	7.16 0.12	6.167e-02 3.157e-03	160.08 2.89	12	0.297	3270
88562	1445.05 8.53	45781.71 35.50	0.204 0.017	11.79 0.10	353.43 7.84	6.98 0.12	4.787e-02 2.590e-03	135.77 2.56	23	0.442	3253
100503	554.41 1.91	46144.83 54.82	0.061 0.045	-8.9 0.15	358.06 34.83	5.80 0.24	1.116e-02 1.366e-03	44.12 1.81	16	0.549	3271
120620	217.18 0.08	48831.22 27.42	0.010 0.009	33.21 0.09	172.87 45.50	14.06 0.11	6.226e-02 1.485e-03	41.98 0.33	28	0.421	3253
123949	9200.0 -	49144.96 62.89	0.972 0.057	-10.82 0.26	128.51 49.01	20.45 >	1.055e-01 >	606.86 122.42	25	0.301	4396
154430	1668.11 17.36	47442.02 76.79	0.108 0.031	-38.14 0.14	312.00 16.55	5.85 0.19	3.400e-02 3.315e-03	133.30 4.53	15	0.480	3058
196445	3221.35 43.00	46037.95 64.62	0.237 0.023	-25.53 0.09	335.85 5.31	4.66 0.11	3.101e-02 2.226e-03	200.46 5.42	12	0.226	3306
211954	5000.0 -	45497.96 149.37	0.391 0.080	-6.08 0.13	64.32 10.07	3.47 0.31	1.686e-02 4.934e-03	219.33 21.40	14	0.353	4081
+38° 118 (a+b)	299.37 0.19	47624.61 3.15	0.144 0.013	-18.68 0.06	132.44 3.93	7.76 0.08	1.406e-02 4.205e-04	31.60 0.32	30	0.303	4260
+38° 118 (ab+c)	3876.66 112.24	46757.73 136.54	0.208 0.062	-18.32 0.09	91.17 14.56	1.65 0.11	1.704e-03 3.616e-04	86.23 6.54	30	0.293	4260
-42° 2048	3259.96 28.30	46948.95 142.67	0.080 0.016	40.52 0.08	188.85 16.40	5.79 0.11	6.496e-02 3.711e-03	258.56 5.36	12	0.239	3270
-64° 4333 CpD	386.04 0.48	47486.99 31.72	0.031 0.012	8.33 0.19	85.40 29.51	11.96 0.20	6.840e-02 3.426e-03	63.43 1.06	16	0.314	3309
Lü 163	965.15 16.01	47283.53 350.26	0.035 >	2.78 0.16	351.32 132.49	3.06 0.22	2.879e-03 6.199e-04	40.64 2.99	14	0.572	4036

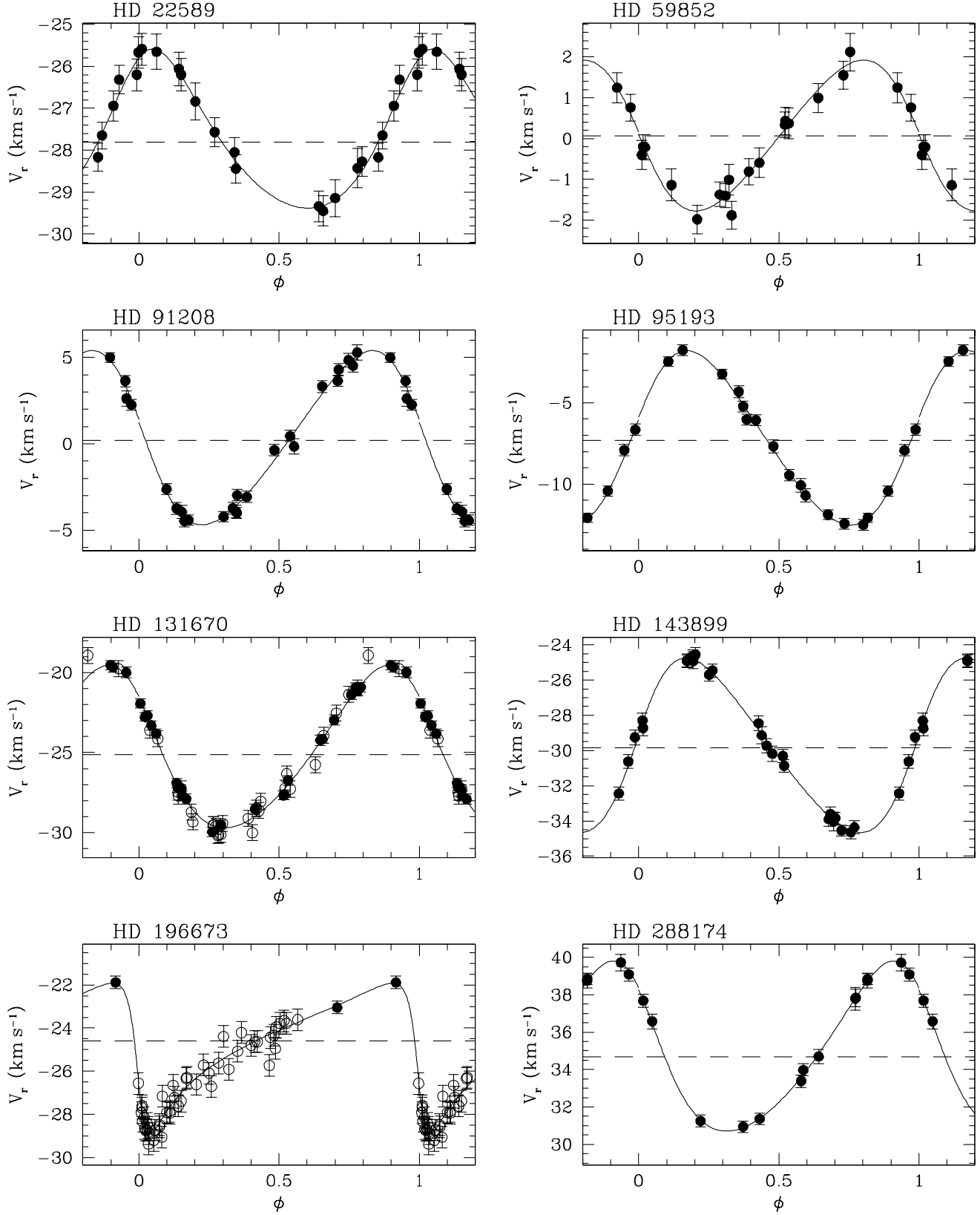


Fig. 3. Phase-folded radial-velocity curves for mild barium stars with orbital solutions. Open circles are for DAO measurements. Two new CORAVEL measurements allow us to propose a new minimum-period estimate for HD 196673. Long-period stars without orbital solutions have their radial velocities displayed as a function of Julian dates

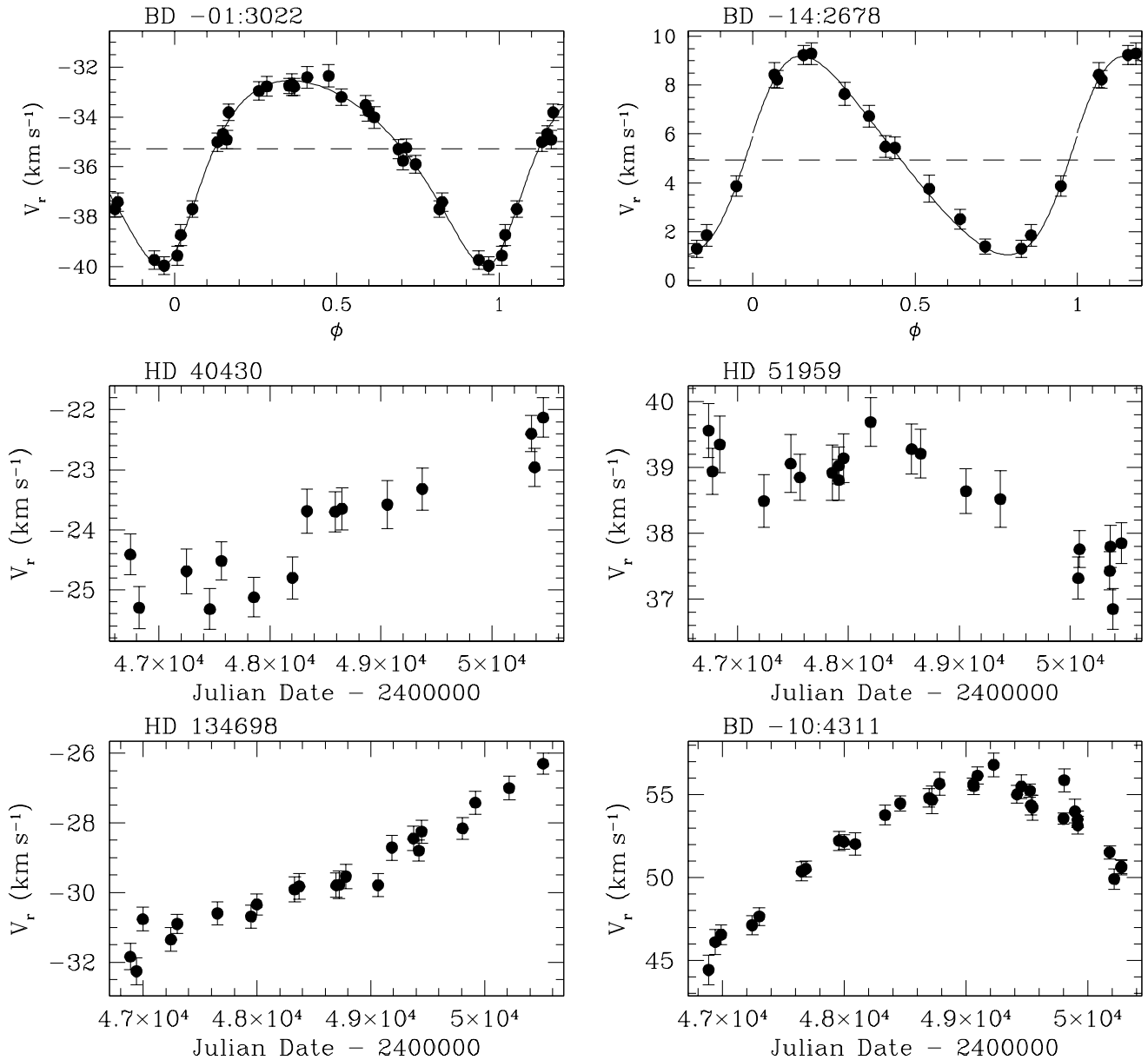


Fig. 3. (continued)

1971), the slightly ‘eccentric’ orbit has been listed, because in the case of barium stars, there is no *physical* argument to prefer the circular orbit (see Jorissen et al. 1998). The corresponding radial-velocity measurements folded in phase are displayed in Fig. 2.

BD +38°118 is a triple hierarchical system. The long-period orbit (noted ab+c) describes the motion of the c component, relatively to the center of mass of the close (short-period) system (noted a+b). The orbits are obtained iteratively by correcting the short-period orbital motion from the long-period perturbation.

4.2. Mild barium stars

Orbital elements were derived for 10 among the 14 mild barium stars presented in this section (Table 6), the others only allowing minimum period estimates. The corresponding phase-folded curves are displayed in Fig. 3, along with the temporal radial-velocity variations of the remaining 4 stars with no orbital solution.

The star HD 196673 deserves a special note. It belongs to the DAO sample with a spectroscopic orbit published by McClure & Woodsworth (1990). However, as shown by 2 new CORAVEL measurements, the inferred orbital period ($P = 4000\text{d}$) was too short. Based on all the DAO+CORAVEL measurements, we propose a new period

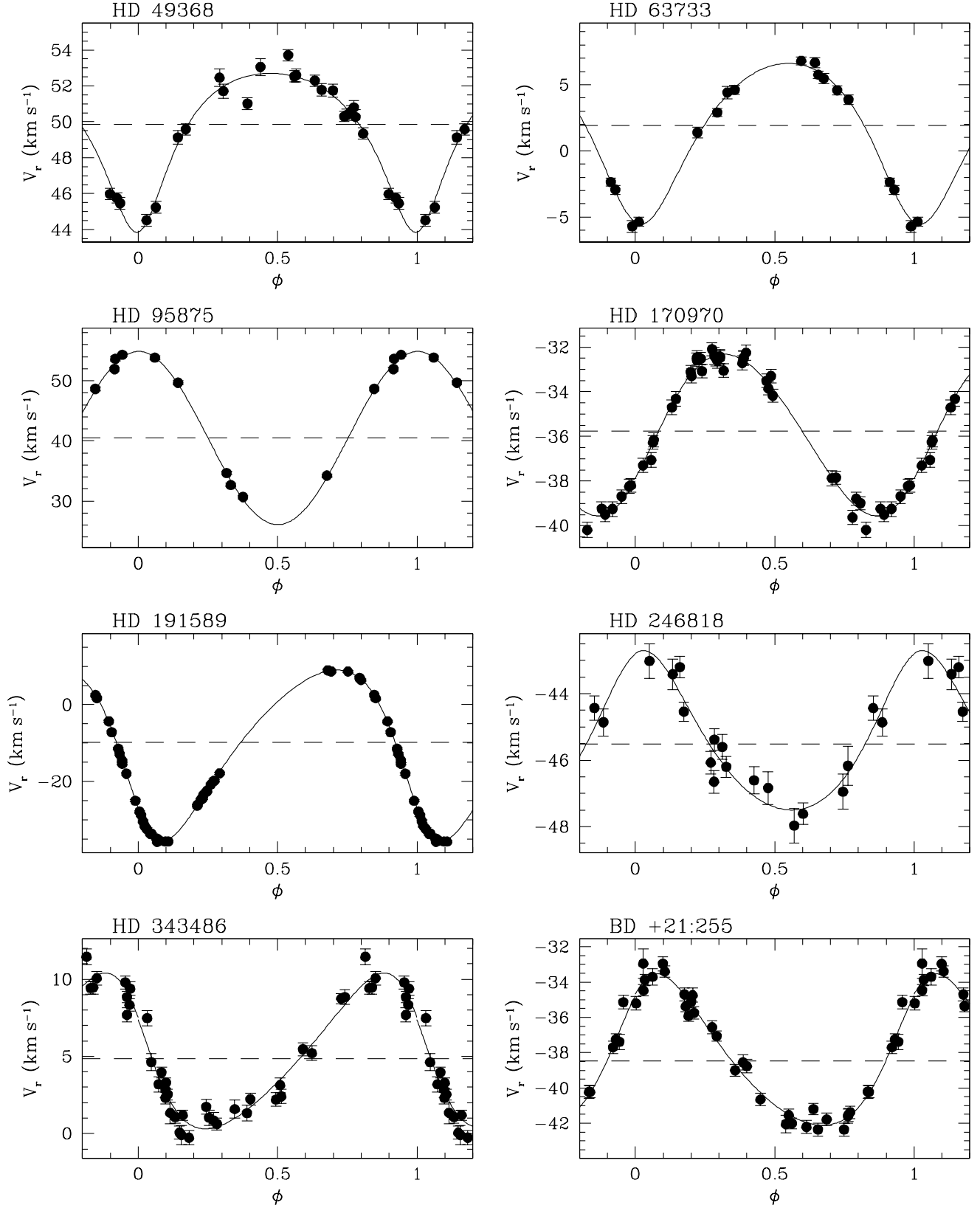


Fig. 4. Phase-folded radial-velocity curves of the photometrically non-variable S stars with orbital solutions. Long-period stars without orbital solutions have their radial velocities displayed as a function of Julian dates

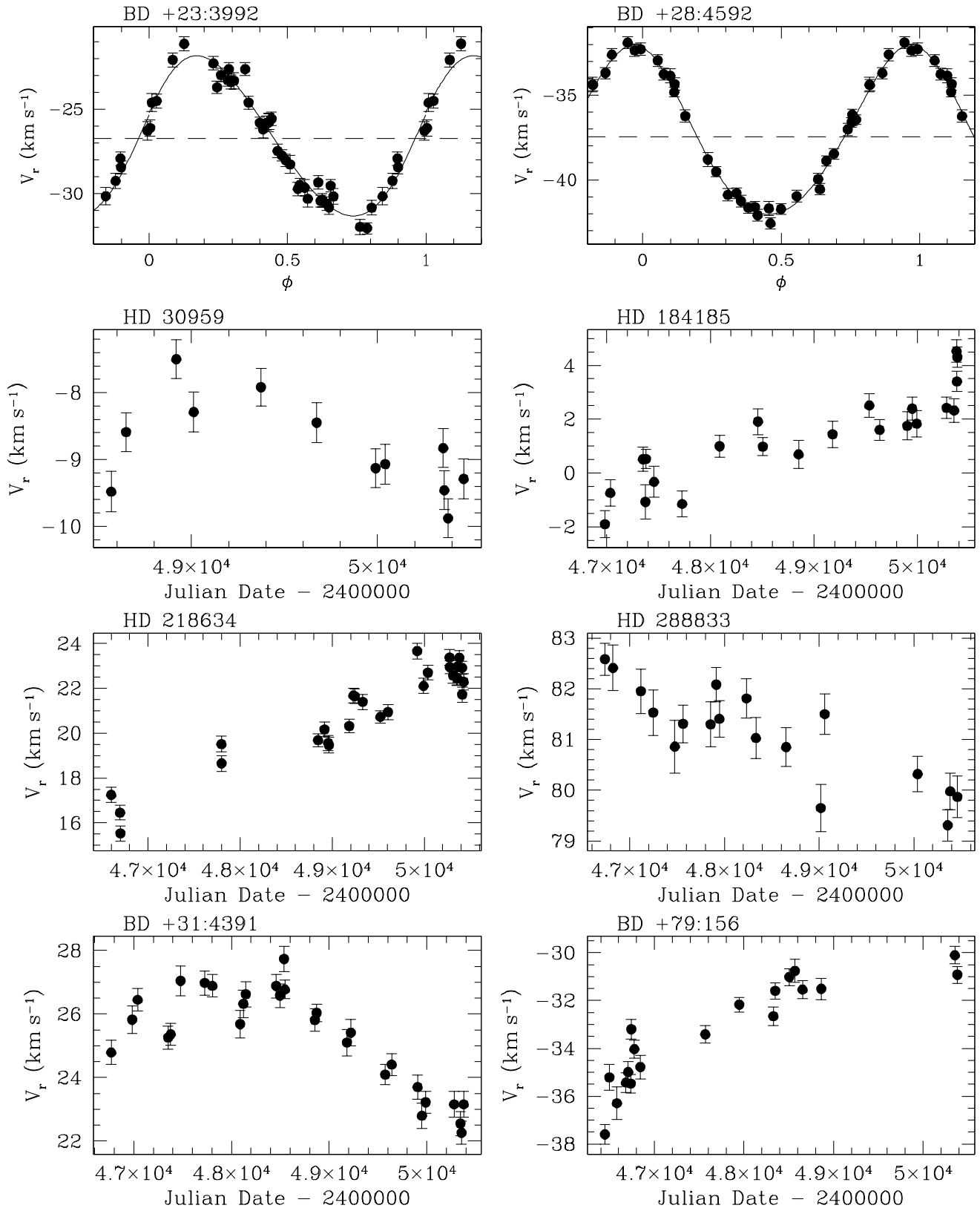


Fig. 4. (continued)

Table 6. Orbital elements for mild barium stars. No uncertainties are given for fixed parameters. N is the number of measurements used to derive the orbital solution and $O - C$ the residue around this solution. ΔT is the span of the observations

Id HD/DM	P [days]	T [HJD −2400000]	e	γ [km s ^{−1}]	ω [deg]	K [km s ^{−1}]	$f(m)$	$a \sin i$ [Gm]	N	$O - C$ [km s ^{−1}]	ΔT [days]
22589	5721.181 453.986	48674.73 133.44	0.240 0.175	−27.97 0.62	341.09 17.38	1.97 0.28	4.180e-03 2.471e-03	150.74 63.26	19	0.217	3641
40430	$P > 3700$								15		3720
51959	$P > 3700$								21		3720
59852	3463.906 53.776	46841.03 187.14	0.152 0.057	0.07 0.07	88.83 20.68	1.85 0.12	2.190e-03 4.376e-04	86.98 5.93	19	0.273	3643
91208	1754.002 13.321	45628.36 54.16	0.171 0.022	0.19 0.08	79.25 10.11	5.05 0.11	2.239e-02 1.555e-03	119.93 2.91	24	0.387	3036
95193	1653.728 8.950	46083.62 38.25	0.135 0.017	−7.32 0.07	283.23 7.60	5.37 0.10	2.585e-02 1.446e-03	120.97 2.34	18	0.264	2596
131670	2929.730 12.265	46405.11 44.96	0.162 0.014	−25.13 0.05	49.88 5.44	5.16 0.08	4.005e-02 1.830e-03	204.94 3.22	55	0.363	5865
134698	$P > 3600$								22		3630
143899	1461.608 6.919	46243.43 19.76	0.194 0.025	−29.83 0.06	277.66 4.57	4.95 0.10	1.740e-02 1.065e-03	97.64 2.04	26	0.271	2649
196673	6500.0 –	43953.72 26.79	0.645 0.028	−24.61 0.10	111.06 4.48	3.49 0.17	1.274e-02 2.175e-03	237.99 13.54	51	0.468	5971
288174	1824.286 7.057	47157.62 17.73	0.194 0.015	34.67 0.04	48.33 3.95	4.55 0.07	1.684e-02 7.431e-04	111.96 1.70	14	0.147	3296
−01°3022	3252.530 31.420	46817.14 34.35	0.285 0.018	−35.38 0.06	212.09 4.31	3.76 0.09	1.586e-02 1.185e-03	161.34 4.28	26	0.253	3667
−10°4311	$P > 3400$								33		3392
−14°2678	3470.519 107.690	48828.06 107.22	0.217 0.040	4.93 0.12	282.61 12.16	4.07 0.14	2.252e-02 2.501e-03	189.38 8.94	15	0.390	3295

(fixed to $P = 6500$ d), which is a lower bound to the actual period. The new preliminary orbital elements obtained by fixing the period to the above value are listed in Table 6.

4.3. Photometrically non-variable S stars

Among the 16 binary S stars with no photometric variations presented in this subsection, an orbital solution has been derived for 10 of them whereas 6 have only minimum-period estimates. The results are given in Table 7. The corresponding phase diagrams are displayed in Fig. 4.

Note that BD +21°255 is a visual binary, most probably of optical nature (Jorissen & Mayor 1992). Table 7 and Fig. 4 provide the orbit of the S star (BD +21°255 = PPM 91178 = SAO 75009 = HIC 8876), whereas the visual K-type companion (BD +21°255p = PPM 91177 = SAO 75008) is also a spectroscopic binary whose orbit is given in Jorissen & Mayor (1992).

The jitter level of the non-binary stars of the sample is of the order of 1-2 km s^{−1} (Jorissen et al. 1998). Its hampering influence on the detection of binarity is thus limited to low-amplitude orbital motions.

5. Mira S stars, SC and C stars: intrinsic radial-velocity variations versus orbital motion

5.1. Intrinsic radial-velocity variations of Mira variables

The large velocity jitter observed in Mira S stars (Tables 3d, 3e and 4 in Jorissen et al. 1998) is related to their complex and variable cc-dips (Barbier et al. 1988). In some cases like for the star χ Cyg, the cc-dip has an inverse P -Cygni shape (Fig. 5a), out of which a meaningful radial velocity is very difficult to extract. In other cases like AA Cyg and R Hya, the cc-dips are featureless, broad and very stable, and these stars have the smallest jitter in our sample of Mira S stars (Table 3d of Jorissen et al. 1998). For stars like R And (=HD 1967) and RZ Peg (=HD 209890), two clearly distinct dips are present. In RZ Peg for example (Figs. 5c-d), the two dips correspond to velocities of −25 and −50 km s^{−1}, whereas the center of mass of the star (as probed by submm observations of the circumstellar CO rotational lines) moves with a velocity of −35 km s^{−1} (Sahai & Liechti 1995), close to the average of the two CORAVEL dips. The two minima observed in the cc-dip are therefore likely associated with upwards- and downwards-moving layers forming a shock in the Mira atmosphere (e.g. Fox et al. 1984, Querci 1986, Bowen 1988, Bessell et al. 1996). The respective weights of the two minima vary with time, and so does the velocity of the resulting blend to which a gaussian is fitted.

Table 7. Orbital elements for the S stars with no (strong) light variations. The symbol $>$ is used for uncertainties exceeding the parameter values in case of badly constrained orbits. N is the number of measurements used to derive the orbital solution and $O - C$ the residue around this solution. ΔT is the span of the observations

Id HD/DM	P [days]	T [HJD −2400000]	e	γ [km s ^{−1}]	ω [deg]	K [km s ^{−1}]	$f(m)$	$a \sin i$ [Gm]	N	$O - C$ [km s ^{−1}]	ΔT [days]
30959	$P > 1900$								12		1895
49368	2995.903 67.152	45145.37 65.01	0.357 0.048	49.85 0.13	184.37 7.27	4.43 0.20	2.201e-02 3.083e-03	170.39 8.73	23	0.577	3635
63733	1160.701 8.922	45990.92 42.60	0.231 0.034	1.91 0.12	168.22 8.91	6.08 0.21	2.492e-02 2.628e-03	94.38 3.39	14	0.379	2685
95875	197.236 0.365	48843.35 91.98	0.023 >	40.61 1.06	25.86 >	14.21 2.12	5.878e-02 9.405e-03	38.54 2.06	10	0.699	1826
170970	4391.997 201.991	48213.21 277.15	0.084 0.043	−35.77 0.06	237.10 24.40	3.62 0.09	2.133e-02 1.856e-03	217.58 11.35	39	0.332	3463
184185	$P > 3400$								22		3403
191589	377.342 0.138	48844.02 0.99	0.253 0.003	−9.74 0.08	128.63 1.15	22.30 0.09	3.937e-01 5.052e-03	111.96 0.48	41	0.292	1895
218634	$P > 3700$								28		3780
246818	2548.543 73.188	47115.84 234.81	0.182 0.111	−45.52 0.19	344.20 35.59	2.40 0.34	3.473e-03 1.494e-03	82.66 12.06	17	0.595	3718
288833	$P > 3900$								18		3721
343486	3165.723 37.626	46880.50 89.02	0.241 0.035	4.86 0.15	65.93 10.78	5.05 0.20	3.862e-02 4.804e-03	213.21 9.16	37	0.823	3398
+21° 255	4137.166 316.831	43578.31 260.49	0.209 0.043	−38.48 0.27	316.59 11.95	4.29 0.16	3.178e-02 4.321e-03	238.82 20.36	36	0.511	4068
+23° 3992	3095.574 41.740	45365.62 177.00	0.105 0.034	−26.72 0.12	286.42 19.87	4.75 0.19	3.380e-02 4.011e-03	200.90 8.35	43	0.706	4135
+28° 4592	1252.941 3.538	48161.32 33.83	0.091 0.017	−37.47 0.06	13.80 9.92	5.01 0.08	1.617e-02 8.147e-04	85.97 1.46	34	0.316	3611
+31° 4391	$P > 3600$								28		3607
+79° 156	$P > 3900$								19		3936

Table 8. Orbital or *pseudo*-orbital (pulsational) elements for Mira S stars, SC stars and Tc-poor C stars. The most likely cause of the radial-velocity variations is given in column 2: ‘orb’ for orbital motion and ‘puls’ for intrinsic atmospheric phenomenon. No uncertainties are given for fixed parameters. The symbol $>$ is used for uncertainties exceeding the parameter values in case of badly constrained orbits. N is the number of measurements used to derive the orbital solution and $O - C$ the residue around this solution. ΔT is the span of the observations

HD/DM GCVS	Var	P_{phot} [days]	P_{orb} [days]	T [HJD −2400000]	e	γ [km s ^{−1}]	ω [deg]	K [km s ^{−1}]	$f(m)$	N	$O - C$ [km s ^{−1}]	ΔT [days]
76221 X Cnc	orb?	~ 195	491.4 –	48642.17 87.15	0.17 >	−5.96 0.20	258.3 65.1	1.37 0.28	1.270e-02 7.748e-05	15	0.664	2117
110813 S UMa	orb	225.9	592.9 61.8	49120.14 98.27	0.00 –	1.41 3.33	0.0 –	6.26 4.25	1.508e-02 3.036e-03	13	1.126	2667
−08° 1900	orb?	~ 59	544.2 5.7	48590.38 33.46	0.55 –	72.257 0.33	216.8 15.3	3.24 0.85	1.119e-02 8.841e-04	17	0.732	3619
54300 R CMi	puls	337.8	337.3 1.3	48693.12 10.20	0.39 0.08	44.03 0.62		8.04 0.77		16	1.836	3740
108105 SS Vir	puls	~ 364	361.2 3.4	50199.59 35.94	0.28 0.12	4.06 0.73		4.40 0.48		16	1.429	1976
209890 RZ Peg	puls	438.7	437.3 3.9	48413.34 34.61	0.15 0.10	−32.28 0.52		8.96 0.82		21	2.249	2932

As an illustration, 2 profiles at different phases (ϕ_{RV}) are given in Figs. 5c-d for RZ Peg. The derived *mean* radial velocities are indicated on the figures.

When the CORAVEL cc-dip of RZ Peg is fitted by a *single* gaussian profile, as indicated on Fig. 5, a *pseudo*-orbital solution is found (Table 8), with a period of 437.3 ± 3.9 d. *This radial-velocity period may be identified*

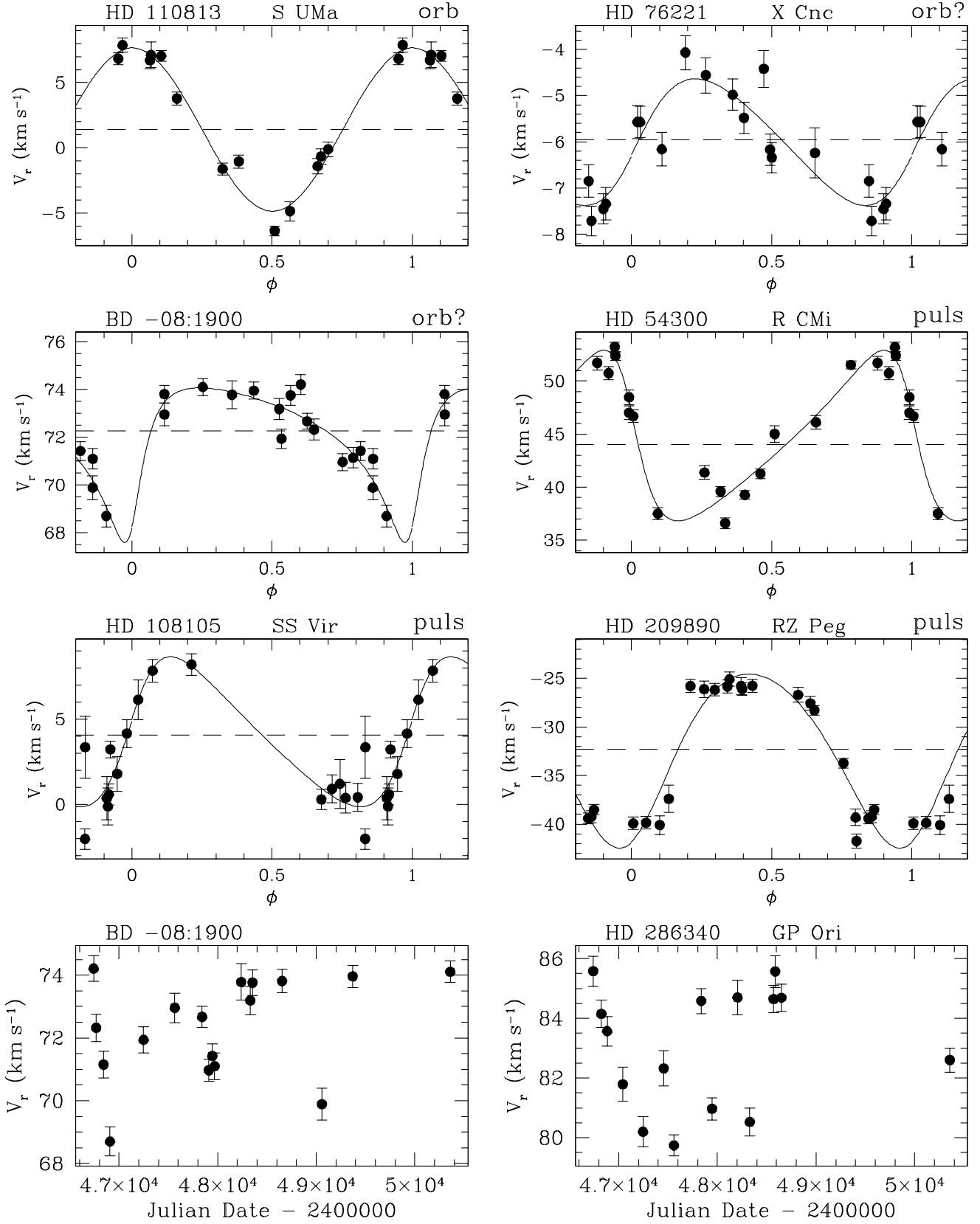


Fig. 6. Phase-folded radial-velocity curves of Mira, SC and S stars with *tentative-* or *pseudo-orbital* solutions. Labels ('orb', 'orb?' or 'puls') are used to characterize our confidence level in the obtained solution or to indicate intrinsic radial-velocity variations. Two stars (BD -08°1900 and HD 286340) have also their radial velocities displayed as a function of Julian dates

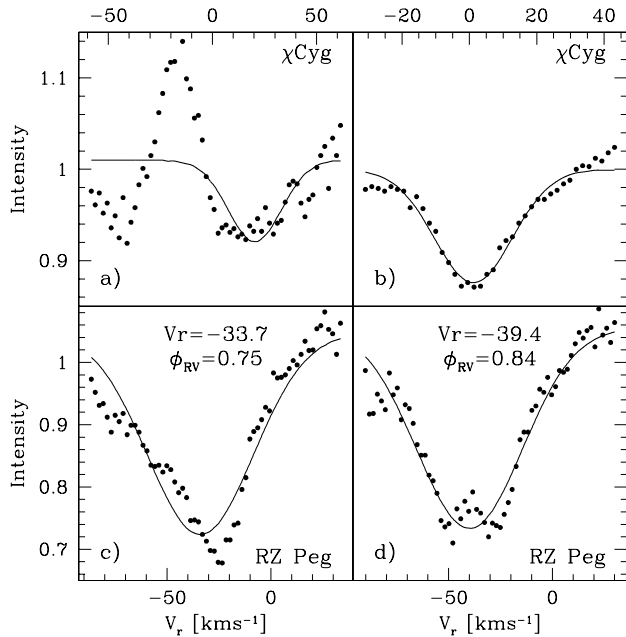


Fig. 5. Examples of cross-correlation dips for Mira S stars. a-b) Profiles for χ Cyg, including an inverse *P Cygni*-like profile; c-d) Two profiles at different phases (ϕ_{RV}) for the star RZ Peg. The time-varying weights of the two minima induce a variation of the measured radial velocity

with the photometric period of 437.8 d derived from the AAVSO light curve for the Mira variations (see Sect. 5.2). It is therefore clear that, although they mimic an orbital motion, the radial-velocity variations of RZ Peg are intrinsic to the Mira phenomenon. They will be discussed in more details in Sect. 5.2. The same coincidence between the periods of the light variations and of the velocity variations is obtained for the CS Mira star R CMi (=HD 54300) and for the C semi-regular (SRa) star SS Vir (=HD 108105) as well. The radial-velocity variations of R CMi can be fitted with a *pseudo-orbital* solution of period 337.3 ± 1.3 d, whereas the GCVS lists $P = 337.8$ d for the associated Mira variations. It is interesting to note that the radial-velocity variations of R CMi are strongly non-sinusoidal in spite of the almost symmetric light curve (the rise time from minimum to maximum light represents 48% of the total cycle, according to the GCVS, compared to 44% for RZ Peg). For SS Vir, the radial-velocity and photometric periods are 361.2 ± 3.4 d and ~ 364 d, respectively. The relevant parameters of the *pseudo-orbits* for RZ Peg, R CMi and SS Vir are given in Table 8. The radial-velocity periods have been used to fold the points in phase. The corresponding diagrams are displayed in Fig. 6.

5.2. Intrinsic radial-velocity variations of Mira S stars: the cases of RZ Peg and χ Cyg

The radial-velocity curve of RZ Peg is well sampled, and makes it possible to investigate in more details the properties of the double cc-dip phenomenon.

Figure 7 presents the evolution of the CORAVEL cross-correlation profiles as a function of the radial-velocity phase (derived from the elements listed in Table 8). The evolution of the profiles, from a single cc-dip to a double cc-dip and *vice versa*, is quite obvious. The radial velocities corresponding to each of the peaks have been extracted by fitting a double-gaussian function to the profile. The resulting velocity curve as a function of the phase is displayed in Fig. 8. Two conclusions may be drawn from this figure: (i) each peak has a rather constant velocity, with the center-of-mass velocity corresponding almost to the average of the two peaks, and (ii) the double dip occurs around velocity phases $\phi_{RV} = 0.7 - 0.9$, and this behaviour repeats from one cycle to the other. The velocity difference between the two peaks is of the order of $20 - 30 \text{ km s}^{-1}$.

The light curve of RZ Peg has been kindly provided to us by the AAVSO (Mattei 1997), and makes it possible to convert velocity phases into photometric phases. The photometric period appears reasonably stable over the time span covered by the radial-velocity observations, with an average period of 437.8 d, very close to the 437.3 d period of the velocity variations. Adopting a period of 437.3 d, the relation $\phi_{\text{phot}} = \phi_{RV} + 0.26$ is derived from the AAVSO maximum (HJD 2 448 301) closest to the zero point of the radial-velocity phase (HJD 2 448 413). From this relation, it may be concluded that *the double cc-dip occurs just after maximum light* ($\phi_{\text{phot}} = 0.0 - 0.2$).

A similar phenomenon of line doubling near maximum light has been reported in several other Mira stars. In the Mira S star χ Cyg, Hinkle et al. (1982) reported such a line doubling for the rotation-vibration second overtone ($\Delta v = 3$) infrared CO lines and high-excitation first overtone ($\Delta v = 2$) CO lines. Maehara (1971) also reported the doubling of CN and atomic lines near 800.0 nm around maximum light in χ Cyg, and Gillet et al. (1985) in S Car. This line-doubling phenomenon is the signature of a shock front propagating through the line-forming region (e.g. Gillet et al. 1985, Bessell et al. 1996). Incidentally, in χ Cyg (Fig. 5), a line-doubling as clear as in RZ Peg is *not* observed for the blue-violet iron lines sampled by CORAVEL (Baranne et al. 1979). The CORAVEL radial velocities of χ Cyg (averaging to $+3.2 \text{ km s}^{-1}$; Table 3d of Jorissen et al. 1998), derived from the clean cc-dips (Fig. 5b), agree with the value obtained by Pierce et al. (1979). Hinkle et al. (1982; their Fig. 15) argue that these blue-violet photospheric absorption lines with a constant radial velocity form in the infalling material for the whole pulsation cycle. Nevertheless, the CORAVEL profile of χ Cyg exhibits some characteristic features that may be

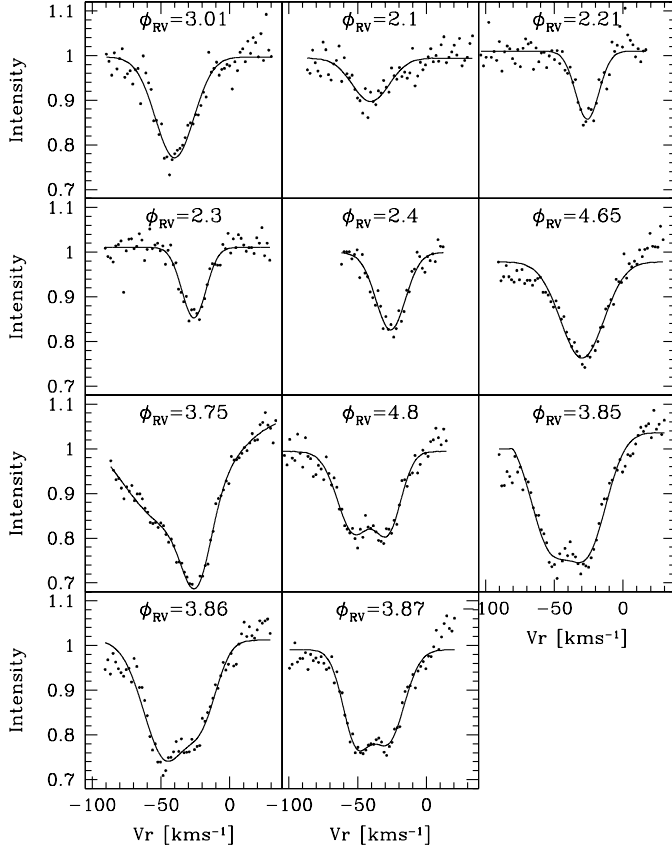


Fig. 7. CORAVEL cc-dips of RZ Peg as a function of the radial-velocity phase (ϕ_{RV}). Phase 0 (HJD 2448 413.3) is close to the epoch of minimum radial-velocity (Fig. 6). The profiles have been fitted with a single or double gaussian function, when appropriate (thin solid line)

related to the shock front propagating through the photosphere. Near visual phases 0.0–0.2, the CORAVEL profile of χ Cyg has a typical inverse *P*-Cygni shape (Fig. 5a) with the blue-shifted ‘emission’ component peaking at -20 km s^{-1} . This velocity corresponds to that of the out-flowing material, as derived from the second overtone CO rotation-vibration lines by Hinkle et al. (1982). A similar inverse *P*-Cygni profile has been reported by Ferlet & Gillet (1984) for the TiI lines near $1 \mu\text{m}$ in Mira near maximum light.

It is very likely that the same physical phenomenon – namely a shock front propagating through the line-forming region – is responsible for the time-dependent features observed in the CORAVEL cc-dips of RZ Peg and χ Cyg. This conclusion is suggested by the fact that in both stars, the line-doubling occurs near maximum light, and the offset between the two distinct components of the cc-dip is of the same order (20 to 30 km s^{-1} , corresponding to the shock discontinuity). These observed features are well reproduced by the synthetic FeI and CO line profiles computed by Bessell et al. (1996) in a dynamical Mira atmosphere with a propagating shock. For some rea-

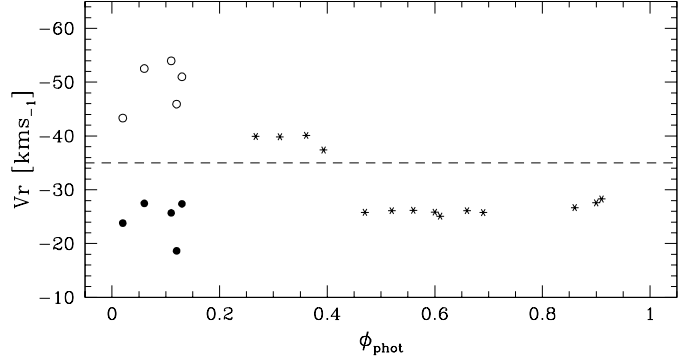


Fig. 8. Radial velocities of RZ Peg as a function of the photometric phase ($\phi_{phot} = \phi_{RV} + 0.26$). Open and filled circles indicate the velocities of the double-line reductions whereas star-like symbols are used for velocities derived from gaussian one-line fitting. The center-of-mass velocity, as probed by submm observations of the CO rotational lines (Sahai & Liechti 1995), is represented by the horizontal dashed line

son however, the atmospheric structures of RZ Peg and χ Cyg must be different, so that only in RZ Peg are the blue-violet iron lines sampled by CORAVEL forming in absorption on both sides of the shock, resulting in a clean double-minima cc-dip.

5.3. Binaries among Mira variables and SC stars

Because they are difficult to observe at minimum light, Mira S and C stars were generally insufficiently sampled to attempt a period search on their radial-velocity curve. Well-sampled curves are, however, available for the Mira S stars AA Cyg, χ Cyg, R Hya, for the C (no Tc) stars SS Vir and S UMa, and for all the SC stars. Some of these stars have already been discussed in Sects. 5.1 and 5.2.

No satisfactory periods emerge for AA Cyg and R Hya. The radial velocity of the absorption lines in χ Cyg is constant, as discussed in Sect. 5.2. The Mira S star S UMa (=HD 110813) is perhaps a binary, since the radial-velocity period $P = 592.2 \text{ d}$ (Table 8) is well distinct from the 225.9 d period of the Mira variations. More measurements are needed, however, before that orbital solution may definitely be accepted.

As far as Tc-poor carbon stars are concerned, X Cnc (= HD 76221) is probably binary, with a 491 d orbit (quite distinct from the -uncertain- 195 d period quoted by the GCVS for the SRb variations).

A possible orbital solution, with $P = 544.2 \pm 5.7 \text{ d}$ and $e = 0.55$, has been found for the SC star BD $-08^\circ 1900$ (Table 8 and Fig. 6). A light curve for this star is provided by Jorissen et al. (1997), who find photometric variations on a time scale of about 59 d . The absence of coincidence between the radial-velocity and photometric (quasi-)periods may lend some credit to the orbital nature of the radial-velocity variations observed for BD $-08^\circ 1900$. We do not accept this interpretation, however, without

the following word of caution: another SC star, GP Ori (=HD 286340), exhibits radial-velocity variations of a nature very similar to those of BD $-08^{\circ}1900$ (Fig. 6; note especially the drift observed in the early phase of the monitoring, reminiscent of that observed for BD $-08^{\circ}1900$), but no orbital solution could be obtained for GP Ori. At this point, we cannot exclude the possibility that the ‘orbital’ solution found for BD $-08^{\circ}1900$ is simply a consequence of a favourable time sampling of irregular, intrinsic variations. One should note in that respect that the σ_V/σ_{V_r} ratio observed for BD $-08^{\circ}1900$ fits well the predictions of a simple linear model of adiabatic acoustic oscillations (Jorissen et al. 1997). Finally, the orbital parameters of BD $-08^{\circ}1900$ would locate that star in a unusual region of the $(e, \log P)$ diagram (Fig. 4 of Jorissen et al. 1998), which is another argument against that orbital solution.

In fact, relatively large-amplitude radial-velocity variations (σ_{V_r} of a few km s^{-1} ; Table 3e of Jorissen et al. 1998) are a common feature among SC stars. For the two Mira SC stars in our sample (R CMi and RZ Peg), periodic radial-velocity variations were found with the same period as the light curve (Sect. 5.1). For the remaining SC stars, which are of semiregular (SR) or irregular (L) variability types, very irregular radial-velocity variations are indeed observed, with the possible exception of BD $-08^{\circ}1900$ discussed above. When the number of measurements is relatively small (< 10) and covers a limited time span, these variations may mimic orbital variations.

Acknowledgements. We thank the AAVSO for communicating us the light curve of RZ Peg. This research has been supported partly by the *Fonds National de la Recherche Scientifique* (Switzerland, Belgium) and the University of Geneva (Geneva Observatory). S.V.E. is supported by a F.R.I.A. doctoral grant (Belgium). A.J. is Research Associate (F.N.R.S., Belgium).

References

- Ake T.B., 1997. In: Wing R. (ed.) *The Carbon Star Phenomenon* (IAU Symp. 177). Kluwer, Dordrecht, in press
- Baranne A., Mayor M., Poncet J.L., 1979, *Vistas in Astron.* 23, 279
- Barbier M., Mayor M., Mennessier M.O., Petit H., 1988, *A&AS* 72, 463
- Bessell M.S., Scholz M., Wood P.R., 1996, *A&A* 307, 481
- Bowen G.H., 1988, *ApJ* 329, 299
- Carquillat J.M., Jorissen A., Udry S., Ginestet N., 1998, *A&A*, in press
- Dominy J.F., Lambert D.L., 1983, *ApJ* 270, 180
- Duquennoy A., Mayor M., Halbwachs J.-L., 1991, *A&AS* 88, 281
- Ferlet R., Gillet D., 1985, *A&A* 133, L1
- Fox M.W., Wood P.R., Dopita M.A., 1984, *ApJ* 286, 337
- Gillet D., Maurice E., Bouchet P., Ferlet R., 1985, *A&A* 148, 155
- Griffin R.F., 1991, *The Observatory* 111, 29
- Griffin R.F., Jorissen A., Mayor M., 1996, *The Observatory* 116, 298
- Han Z., Eggleton P.P., Podsiadlowski P., Tout C.A., 1995, *MNRAS* 277, 1443
- Hinkle K.H., Hall D.N.B., Ridgway S.T., 1982, *ApJ* 252, 697
- Jorissen A., 1997. In: Mikolajewska J. (ed.) *Physical Processes in Symbiotic Stars and Related Systems*. Copernicus Foundation for Polish Astronomy, Warsaw, p.135
- Jorissen A., Mayor M., 1988, *A&A* 198, 187
- Jorissen A., Mayor M., 1992, *A&A* 260, 115
- Jorissen A., Manfroid J., Sterken C., 1991, *The Messenger* 66, 53
- Jorissen A., Hennen O., Mayor M., Bruch A., Sterken C., 1995, *A&A* 301, 707
- Jorissen A., Mowlavi N., Sterken C., Manfroid J., 1997, *A&A* 324, 578
- Jorissen A., Van Eck S., Mayor M., Udry S., 1998, *A&A*, in press
- Kholopov P.N., Samus' N.N., Frolov M.S., et al., 1985. *General Catalogue of Variable Stars* (4th edition). Nauka, Moscow
- Kukarkin B. V., Kholopov P. N., Artiukhina N. M., et al., 1982. *New General Catalogue of Suspected Variable Stars*. Nauka, Moscow
- Lambert D.L., 1985. In: Jascheck M., Keenan P.C. (eds.) *Cool Stars with Excesses of Heavy Elements*. Reidel, Dordrecht, p.191
- Little S.J., Little-Marenin I.R., Hagen-Bauer W., 1987, *AJ* 94, 981
- Lü P.K., 1991, *AJ* 101, 2229
- Lü P.K., Dawson D.W., Upgren A.R., Weis E.W., 1983, *ApJS* 52, 169
- Lucy L.B., Sweeney M.A., 1971, *AJ* 76, 544
- Maehara H., 1971, *PASJ* 23, 503
- Mattei J.A., 1997. *Observations from the AAVSO International Database*, private communication
- McClure R.D., 1983, *ApJ* 268, 264
- McClure R.D., Woodsworth A.W., 1990, *ApJ* 352, 709
- McClure R.D., Fletcher J.M., Nemec J.M., 1980, *ApJ* 238, L35
- Mermilliod J.-C., Mermilliod M., Hauck B., 1997, *A&AS* 124, 349
- Pierce J.N., Willson L.A., Beavers W.I., 1979, *PASP* 91, 372
- Querci M., 1986. In: H.R. Johnson, F. Querci (eds.) *The M-Type Stars* (Monograph Series on Nonthermal Phenomena in Stellar Atmospheres). NASA SP-492, NASA & CNRS, Washington D.C., p. 113
- Sahai R., Liechti S., 1995, *A&A* 293, 198
- Schindler M., Stencel R.E., Linsky J.L., Basri G.S., Helfand D.J., 1982, *ApJ* 263, 269
- Smith V.V., Lambert D.L., 1987, *MNRAS* 226, 563
- Stephenson C.B., 1984. *The General Catalogue of Galactic S Stars*, Publ. Warner & Swasey Observ. 3, 1 (GCGSS)
- Udry S., Mayor M., Van Eck S., Jorissen A., Prévot L., Grenier S., Lindgren H., 1998, *A&AS*, in press (Paper II)
- Van Eck S., Jorissen A., Udry S., Mayor M., Pernier B., 1997, *A&A*, in press
- Warner B., 1965, *MNRAS* 129, 263